

Learning Parameters and Constitutive Relationships with Physics Informed Deep Neural Networks

Alexandre M. Tartakovsky^a, Carlos Ortiz Marrero^a, Paris Perdikaris^b, Guzel D.
Tartakovsky^a
^a, David Barajas-Solano^a

Problems

- physical models of many complex natural systems are “partially” known:
 - conservation laws do not provide a closed system of equations.
- Non-homogeneous turbulence, non-Newtonian fluid flow, multiphase flow and transport in porous media, and granular materials:
 - accurate theoretical closures are not available.
- Even when sufficiently accurate closed-form partial differential equations(PDE) models are available:
 - (space-dependent) parameters are typically unknown.

Method

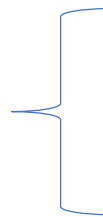
In the most general case, system dynamics can be described as

$$\frac{\partial u}{\partial t} = F(u),$$

F is a function or differential operator

The following equation describes flow in **porous media**

$$\frac{\partial u(\mathbf{x}, t)}{\partial t} = -\nabla \cdot (K(\mathbf{x}, u) \nabla u(\mathbf{x}, t))$$

- 
- $K(\mathbf{x}, u) = K(\mathbf{x})$ a linear diffusion equation with heterogeneous diffusion coefficient $K(\mathbf{x})$
 - $K(\mathbf{x}, u) = K(u)$ a nonlinear diffusion equation with a state-dependent coefficient $K(u)$

Method: physics-informed neural network

differential operator \leftarrow

$$\mathcal{L}[u, K(\mathbf{x}, u)] = 0, \quad \mathbf{x} \in \Omega$$
$$u(\mathbf{x}) = g(\mathbf{x}), \quad \mathbf{x} \in \partial_D \Omega,$$
$$\mathbf{n} \cdot K(\mathbf{x}, u) \nabla u(\mathbf{x}) = q(\mathbf{x}), \quad \mathbf{x} \in \partial_N \Omega.$$

Dirichlet and Neumann boundary conditions \leftarrow

Obviously, we need two neural networks to represent
the state : $u()$ and
the unknown constitutive relationship : $K()$

$$\hat{u}(\mathbf{x}; \theta) = \mathcal{N}\mathcal{N}_u(\mathbf{x}; \theta), \quad \hat{K}(\mathbf{x}, u; \gamma) = \mathcal{N}\mathcal{N}_K(\mathbf{x}, u; \gamma)$$

θ and γ are the DNN parameters

Loss function

$$\mathcal{L}[u, K(\mathbf{x}, u)] = 0$$

$$\mathbf{n} \cdot K(\mathbf{x}, u) \nabla u(\mathbf{x}) = q(\mathbf{x}).$$

Two extra networks represent the eq(1) and eq(3)

$$f(\mathbf{x}; \gamma, \theta) = \mathcal{L}[\mathcal{NN}_u(\mathbf{x}; \theta), \mathcal{NN}_K(\mathbf{x}, \mathcal{NN}_u(\mathbf{x}; \theta); \gamma)] = \mathcal{NN}_f(\mathbf{x}; \theta, \gamma),$$

$$f_N(\mathbf{x}; \gamma, \theta) = \mathbf{n} \cdot \mathcal{NN}_K(\mathbf{x}, \mathcal{NN}_u(\mathbf{x}; \theta); \gamma) \nabla \mathcal{NN}_u(\mathbf{x}; \theta) = \mathcal{NN}_N(\mathbf{x}; \theta, \gamma).$$

The corresponding losses are:

$$\left\{ \begin{array}{l} \frac{1}{N_c} \sum_{i=1}^{N_c} f(\mathbf{x}_i^c; \gamma, \theta)^2 \\ \frac{1}{N_N} \sum_{i=1}^{N_N} [f_N(\mathbf{x}_i^N; \gamma, \theta) - q_i^*]^2 \end{array} \right.$$

Eq(2)'s loss: $u(\mathbf{x}) = g(\mathbf{x}) \longrightarrow \frac{1}{N_D} \sum_{i=1}^{N_D} [\hat{u}(\mathbf{x}_i^D; \theta) - g_i^*]^2$

The two networks'
loss functions:

$$\hat{u}(\mathbf{x}; \theta) = \mathcal{NN}_u(\mathbf{x}; \theta) \longrightarrow \frac{1}{N_u} \sum_{i=1}^{N_u} [\hat{u}(\mathbf{x}_i^u; \theta) - u_i^*]^2$$

$$\hat{K}(\mathbf{x}, u; \gamma) = \mathcal{NN}_K(\mathbf{x}, u; \gamma) \longrightarrow \frac{1}{N_K} \sum_{i=1}^{N_K} [\hat{K}(\mathbf{x}_i^K, \hat{u}(\mathbf{x}_i^K; \theta); \gamma) - K_i^*]^2$$

The final loss function:

$$\begin{aligned} L(\theta, \gamma) = & \frac{1}{N_K} \sum_{i=1}^{N_K} \left[\hat{K}(\mathbf{x}_i^K, \hat{u}(\mathbf{x}_i^K; \theta); \gamma) - K_i^* \right]^2 + \frac{1}{N_u} \sum_{i=1}^{N_u} [\hat{u}(\mathbf{x}_i^u; \theta) - u_i^*]^2 \\ & + \frac{1}{N_D} \sum_{i=1}^{N_D} [\hat{u}(\mathbf{x}_i^D; \theta) - g_i^*]^2 + \frac{1}{N_N} \sum_{i=1}^{N_N} [f_N(\mathbf{x}_i^N; \gamma, \theta) - q_i^*]^2 \\ & + \frac{1}{N_c} \sum_{i=1}^{N_c} f(\mathbf{x}_i^c; \gamma, \theta)^2. \end{aligned}$$

$$(\theta, \gamma) = \arg \min_{\theta, \gamma} L(\theta, \gamma).$$

Optimizer: L-BFGS-B (lower cost than SGD)

Application: a linear diffusion equation

$$\nabla \cdot (K(\mathbf{x})\nabla u(\mathbf{x})) = 0, \quad \mathbf{x} \equiv (x_1, x_2)^T \in (0, 1) \times (0, 1)$$

$$u(\mathbf{x}) = 1, \quad x_2 = 0 \quad \text{and} \quad u(\mathbf{x}) = 0, \quad x_2 = 1$$

$$\frac{\partial u(\mathbf{x})}{\partial x_1} = 0 \quad x_1 = \{0, 1\}.$$

Dirichlet and
Neumann
boundary
conditions

$$f(\mathbf{x}; \gamma, \theta) = \nabla \cdot [\mathcal{N}\mathcal{N}_K(\mathbf{x}; \gamma)\nabla\mathcal{N}\mathcal{N}_u(\mathbf{x}; \theta)] = \mathcal{N}\mathcal{N}_f(\mathbf{x}; \theta, \gamma)$$

$$f_N(\mathbf{x}; \theta) = \partial\mathcal{N}\mathcal{N}_u(\mathbf{x}; \theta)/\partial x_2 = \mathcal{N}\mathcal{N}_N(\mathbf{x}; \theta)$$

This equation describes saturated flow in heterogeneous porous media with hydraulic conductivity $K(\mathbf{x})$

$$\begin{aligned}
L(\theta, \gamma) &= \frac{1}{N_K} \sum_{i=1}^{N_K} \left[\hat{K}(\mathbf{x}_i^K; \gamma) - K_i^* \right]^2 + \frac{1}{N_u} \sum_{i=1}^{N_u} [\hat{u}(\mathbf{x}_i^u; \theta) - u_i^*]^2 \\
&+ \frac{1}{N_D} \sum_{i=1}^{N_D} [\hat{u}(\mathbf{x}_i^D; \theta) - g_i^*]^2 + \frac{1}{N_N} \sum_{i=1}^{N_N} f_N(\mathbf{x}_i^N; \gamma, \theta)^2 \\
&+ \frac{1}{N_c} \sum_{i=1}^{N_c} f(\mathbf{x}_i^c; \gamma, \theta)^2.
\end{aligned}$$

Generating reference data:

K: the Gaussian process (zero mean + $C(\mathbf{x}, \mathbf{x}')$)

u: finite volume (FV) method

$$C(\mathbf{x}, \mathbf{x}') = \sigma^2 \exp(-\|\mathbf{x} - \mathbf{x}'\|^2 / 2\lambda^2) \quad \sigma = 1 \text{ and } \lambda = 0.15$$

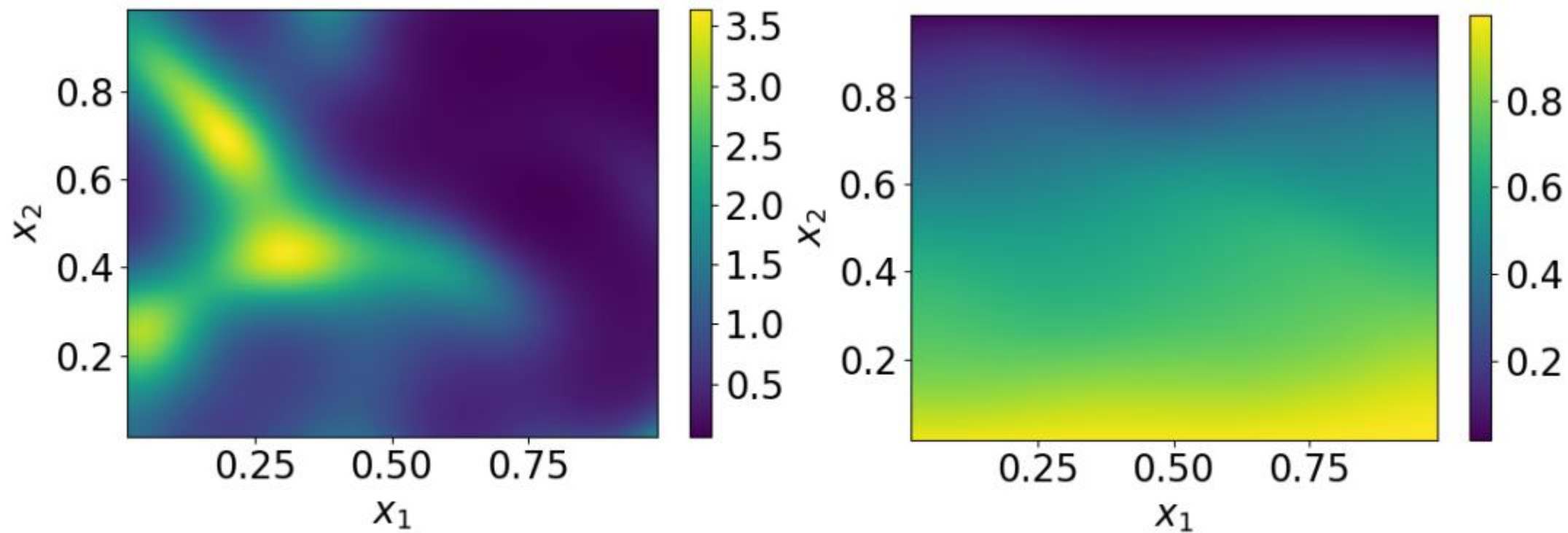


Figure 1: Reference K (left) and u (right) fields.

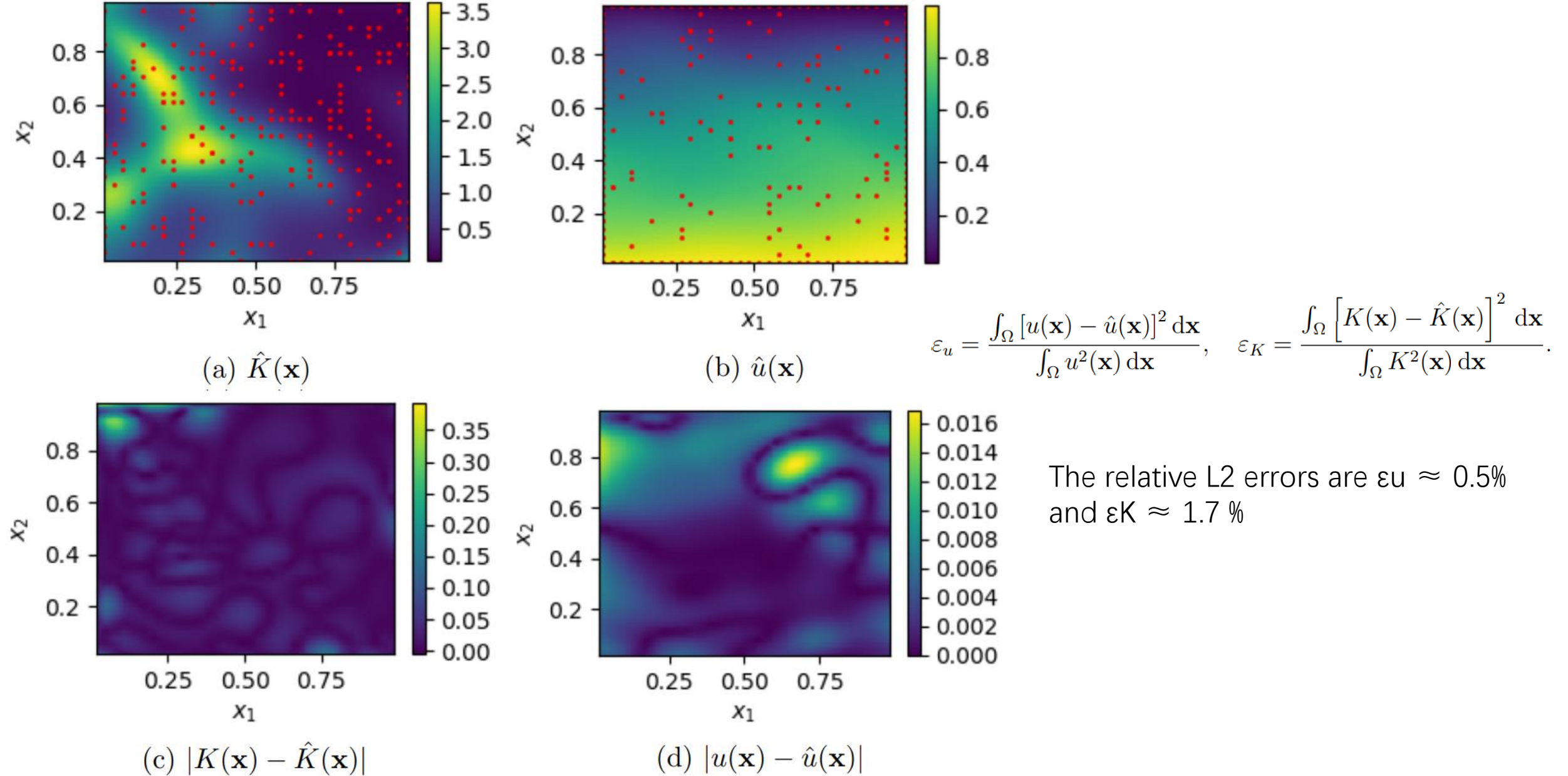
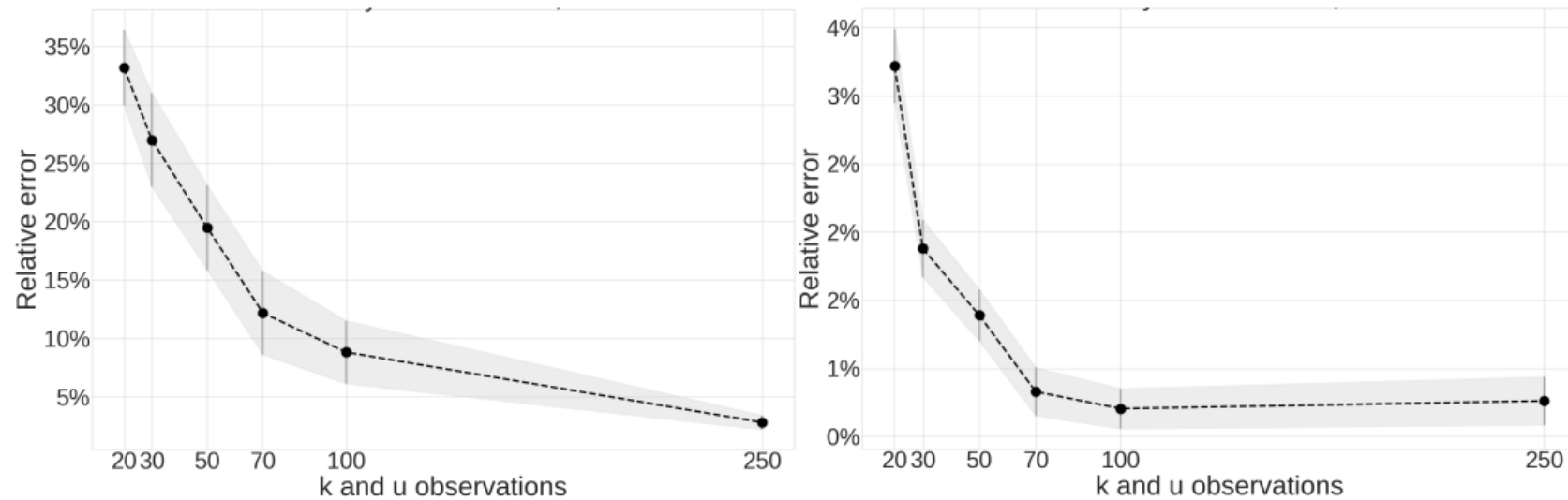


Figure 2: Estimated (a) $\hat{K}(\mathbf{x})$ and (b) $\hat{u}(\mathbf{x})$ fields. The red dots indicate the observation locations. Absolute point errors in (c) $\hat{K}(\mathbf{x})$ and (d) $\hat{u}(\mathbf{x})$. $N_K = 250$, $N_u = 100$, and $N_c = 1024$.

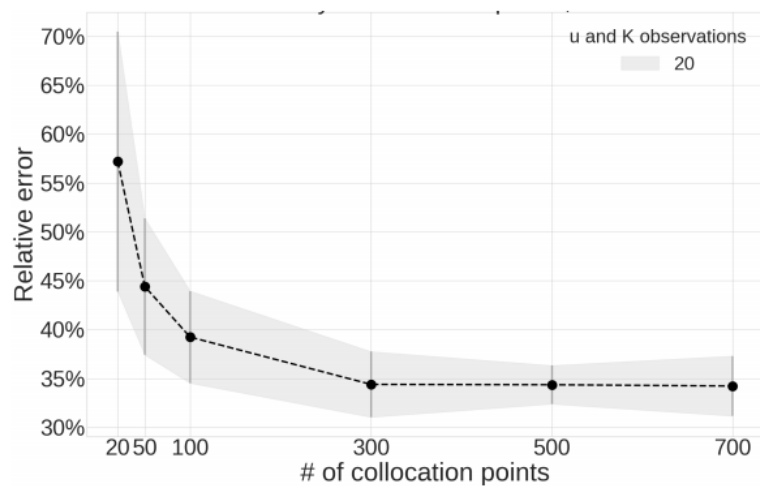
study the effect of DNN initialization on the estimated K and u .

$$\bar{\varepsilon}_{(\cdot)} = \frac{1}{N_s} \sum_{i=1}^{N_s} \varepsilon_{(\cdot),i}, \quad \sigma_{\varepsilon_{(\cdot)}} = \sqrt{\frac{1}{N_s} \sum_{i=1}^{N_s} (\varepsilon_{(\cdot),i} - \bar{\varepsilon}_{(\cdot)})^2},$$

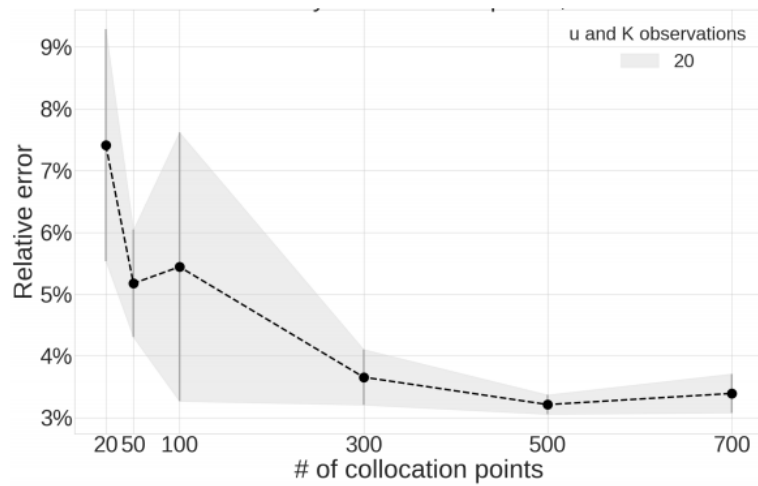


1. uncertainty in \hat{u} is much smaller than in \hat{K}
2. the initialization of the DNNs does not have a significant effect on DNN predictions

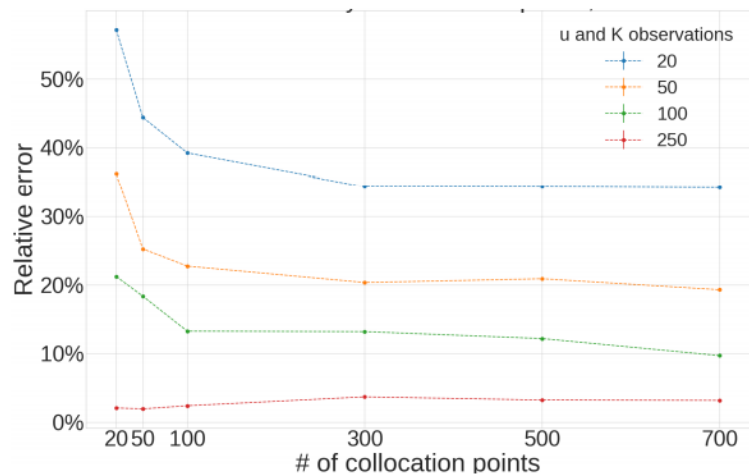
Figure 3: Mean and standard deviation of \hat{K} and \hat{u} obtained with 11 different network initializations using Xavier's initialization scheme as a function of $N = N_K = N_u$. The u and K measurement locations are fixed, and $N_c = 1024$ collocation points are used.



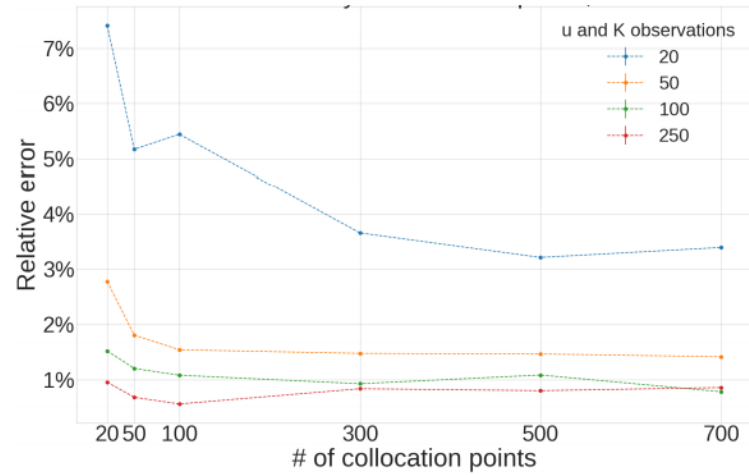
(a) $\bar{\epsilon}_K$ and σ_{ϵ_K}



(b) $\bar{\epsilon}_u$ and σ_{ϵ_u}



(c) $\bar{\epsilon}_K$



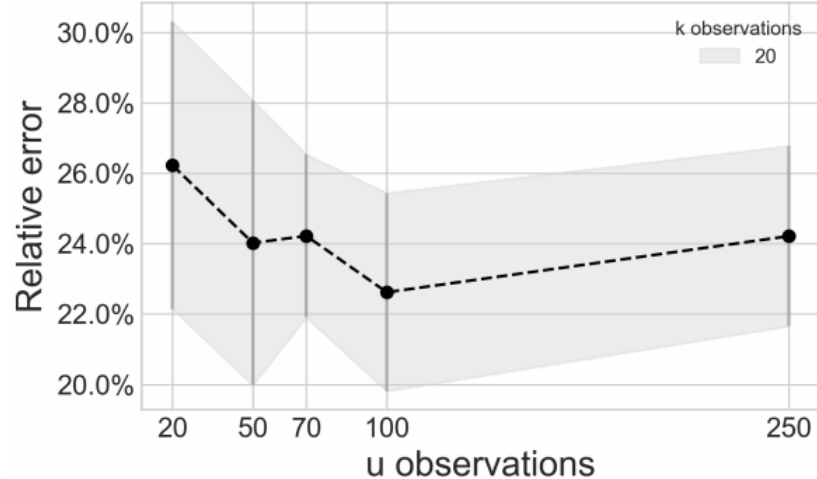
(d) $\bar{\epsilon}_u$

Figure 4: (a)-(b): Mean and standard deviation of the estimated u and K relative errors as a function of the number of collocation points N_c . For a given N_c , the DNNs are trained 11 times for different configurations of collocation points to compute the mean and variance of the relative errors. The u and K measurement locations are fixed, and $N = N_K = N_u = 20$. Shaded area width is equal to two standard deviations. (c)-(d): Mean K and u relative errors as a function of N_c and N .

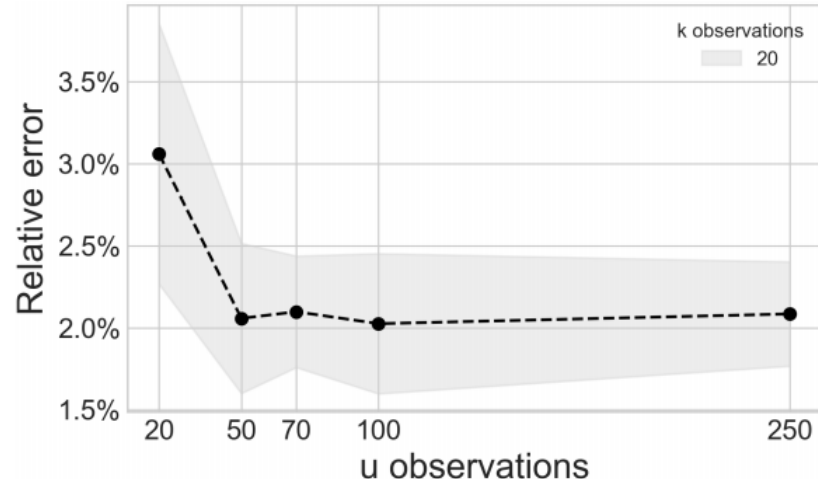
study the effect of the number and location of collocation points

(a),(b): The location of collocation points has a notable effect on the errors, especially for a relatively small N_c

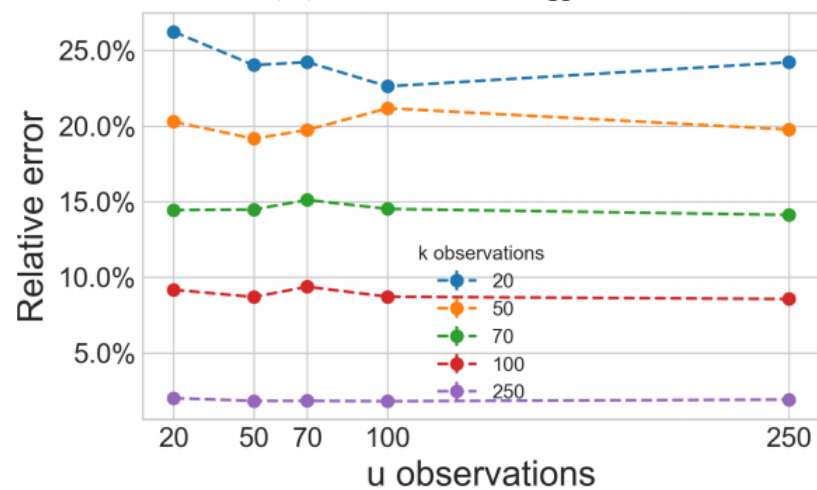
(c),(d): imposing PDE constraints reduces the mean error in K and u by close to 50%



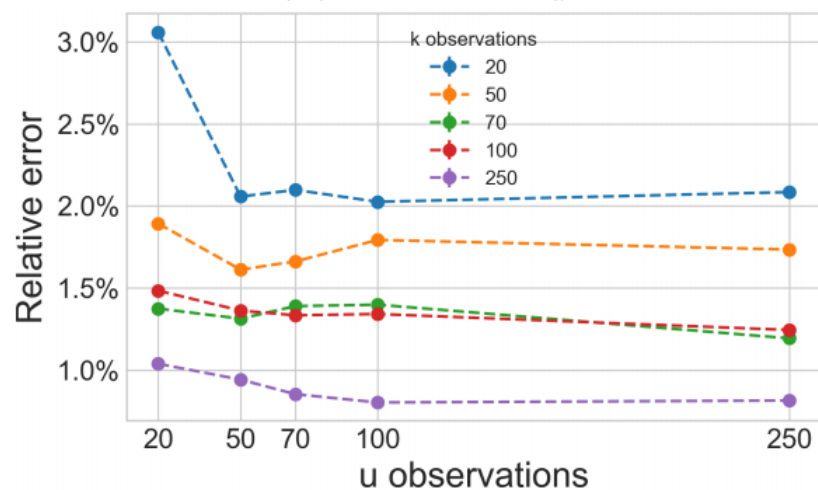
(a) $\bar{\varepsilon}_K$ and σ_{ε_K}



(b) $\bar{\varepsilon}_u$ and σ_{ε_u}



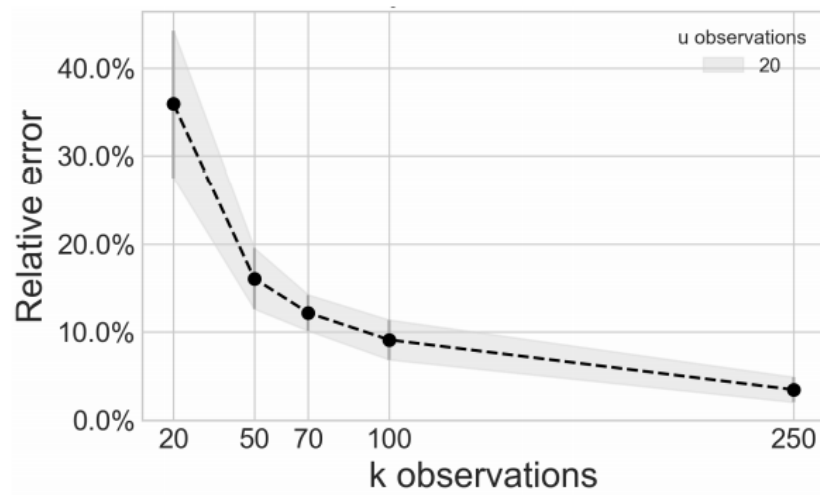
(c) $\bar{\varepsilon}_K$



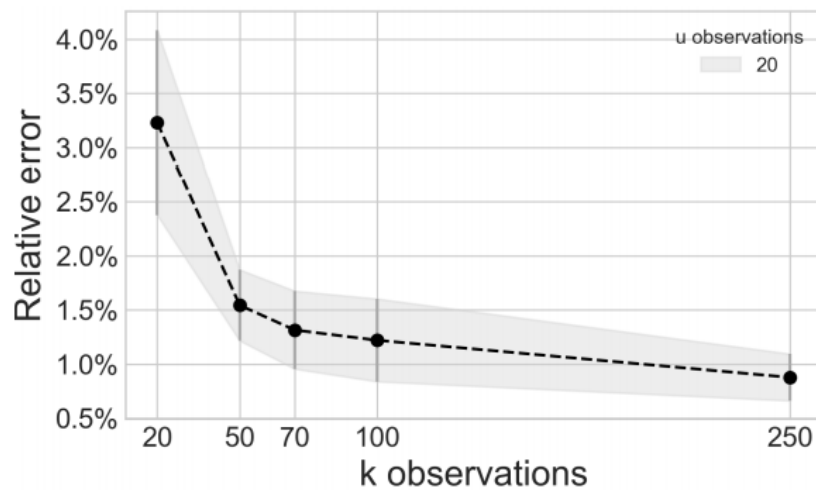
(d) $\bar{\varepsilon}_u$

study how the number of K observations versus the number of u observations affects ε_u and ε_K

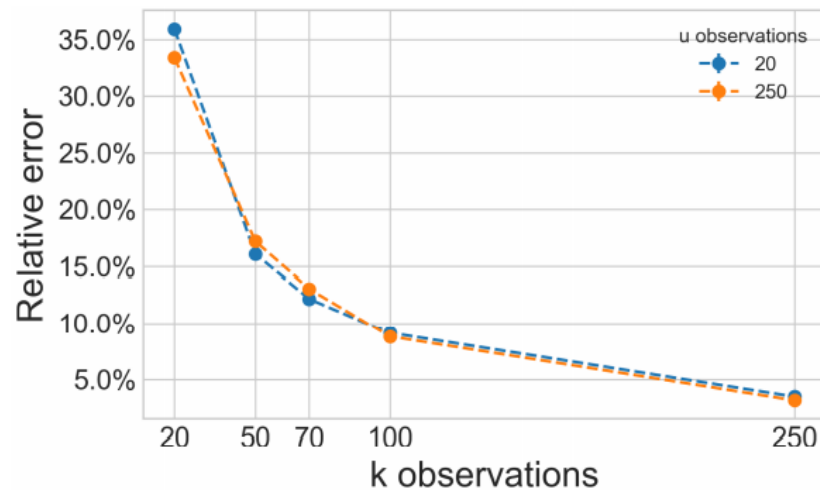
Figure 5: (a) and (b): Mean relative L_2 error of the predicted K and u as a function of the number of u observations. The number of K observations is 20. Shaded area width is equal to two standard deviations computed for 11 different configurations of u observations. (c) and (d): Mean relative L_2 error of the predicted K and u as a function of the number of u and K observations.



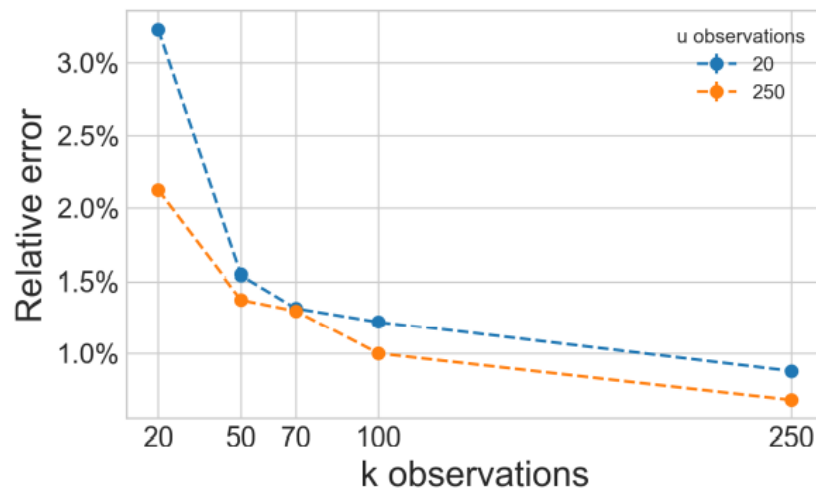
(a) $\bar{\varepsilon}_K$ and σ_{ε_K}



(b) $\bar{\varepsilon}_u$ and σ_{ε_u}



(c) $\bar{\varepsilon}_K$



(d) $\bar{\varepsilon}_u$

Figure 6: (a) and (b): Mean relative L_2 error of the predicted K and u as a function of the number of K observations. The number of u observations is 20. Shaded area width is equal to two standard deviations computed for 11 different configurations of K observations. (c) and (d): Mean relative L_2 error of the predicted K and u as a function of the number of u and K observations.

K measurements are more important than u measurements for reducing error in \hat{K} and \hat{u} .

Compared with MAP

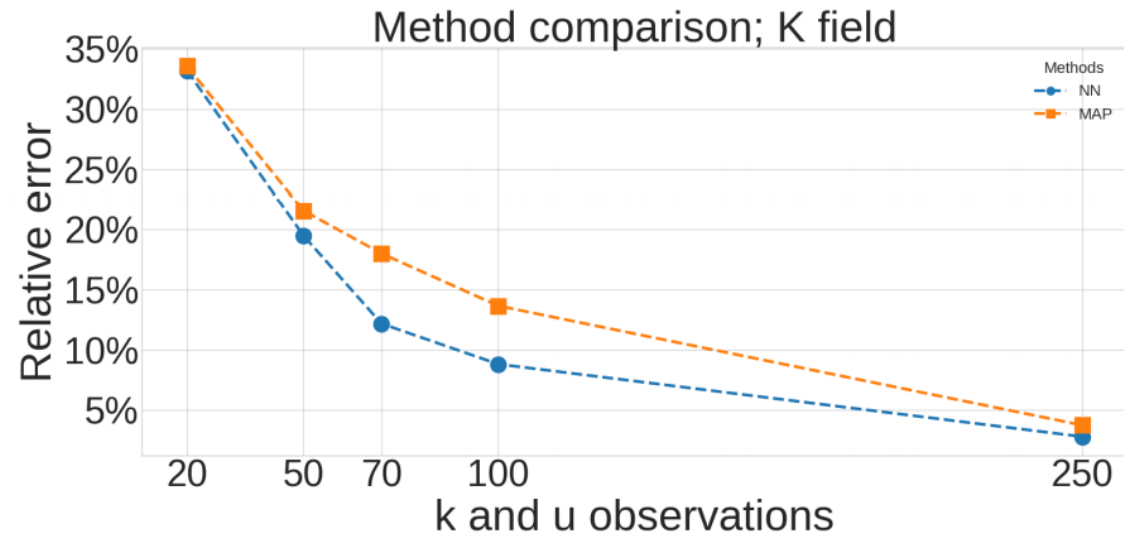


Figure 7: Comparison between L_2 error in the MAP estimate of K and mean L_2 error $\bar{\epsilon}_K$ in the DNN K estimate.

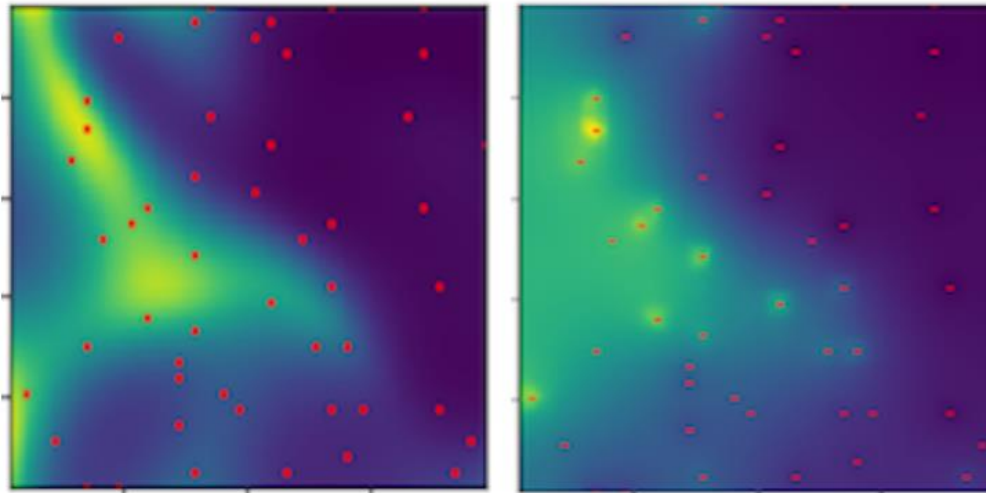


Figure 8: Comparison between the DNN prediction of K (left) and the MAP prediction of K (right) using 50 observations of both u and K .

Application: a nonlinear diffusion equation

$$\nabla \cdot [K(u)\nabla u(\mathbf{x})] = 0, \quad (x_1, x_2) \in (0, L_1) \times (0, L_2)$$

subject to the boundary conditions

$$\begin{aligned} u(\mathbf{x}) &= u_0, & x_1 &= L_1, \\ -K(u)\frac{\partial u(\mathbf{x})}{\partial x_1} &= q, & x_1 &= 0 \\ \frac{\partial u(\mathbf{x})}{\partial x_2} &= 0, & x_2 &= \{0, L_2\}. \end{aligned}$$

1. A two-dimensional horizontal unsaturated flow (flow of water and air) in a homogeneous porous medium
2. $u(x)$ is the water pressure and $K(u)$ is the pressure-dependent partial conductivity of the porous medium
3. no measurements of $K(u)$ are available

$$\hat{u}(\mathbf{x}; \theta) = \mathcal{N}\mathcal{N}_u(\mathbf{x}; \theta), \quad \hat{K}(u; \gamma) = \mathcal{N}\mathcal{N}_K(u; \phi)$$

$$f(\mathbf{x}; \theta, \gamma) = \nabla \cdot [\mathcal{N}\mathcal{N}_K(\mathcal{N}\mathcal{N}_u(\mathbf{x}; \theta); \gamma) \nabla \mathcal{N}\mathcal{N}_u(\mathbf{x}; \theta)] = \mathcal{N}\mathcal{N}_f(\mathbf{x}; \theta, \gamma),$$

$$\mathbf{f}_N(\mathbf{x}; \phi, \gamma) = -\mathcal{N}\mathcal{N}_K(\mathcal{N}\mathcal{N}_u(\mathbf{x}; \theta); \gamma) \nabla \mathcal{N}\mathcal{N}_u(\mathbf{x}; \theta) = \mathcal{N}\mathcal{N}_N(\mathbf{x}; \theta, \gamma),$$

$$\begin{aligned} \mathcal{L}(\theta, \gamma) &= \frac{1}{N_u} \sum_{i=1}^{N_u} [\hat{u}(\mathbf{x}_i^u; \theta) - u_i^*]^2 \\ &+ \frac{1}{N_c} \sum_{i=1}^{N_c} f(\mathbf{x}_i; \theta, \gamma)^2 + \frac{1}{N_D} \sum_{i=1}^{N_D} [\hat{u}(\mathbf{x}_i^D; \theta) - u_0]^2 \\ &+ \frac{1}{N_N^{(x_1)}} \sum_{i=1}^{N_N} \left[f_N^{(x_1)}(\mathbf{x}_i^{N, x_1}; \phi, \gamma) - q \right]^2 + \frac{1}{N_N^{(x_2)}} \sum_{i=1}^{N_N} \left[f_N^{(x_2)}(\mathbf{x}_i^{N, x_2}; \phi, \gamma) \right]^2 \end{aligned}$$

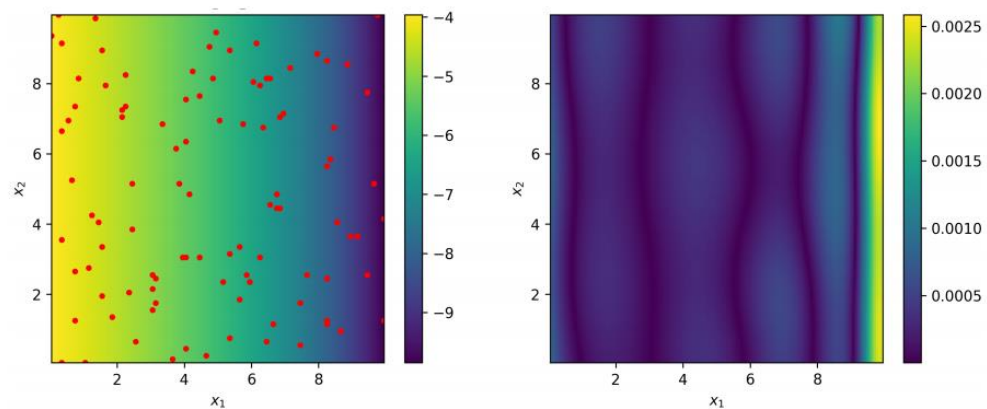


Figure 9: (Left) Referenced $u(\mathbf{x})$ field generated using STOMP with the van Genuchten model for $K(u)$ and the locations of u observations. (Right) Absolute error in the $u(\mathbf{x})$ field estimated with the physics informed DNN.

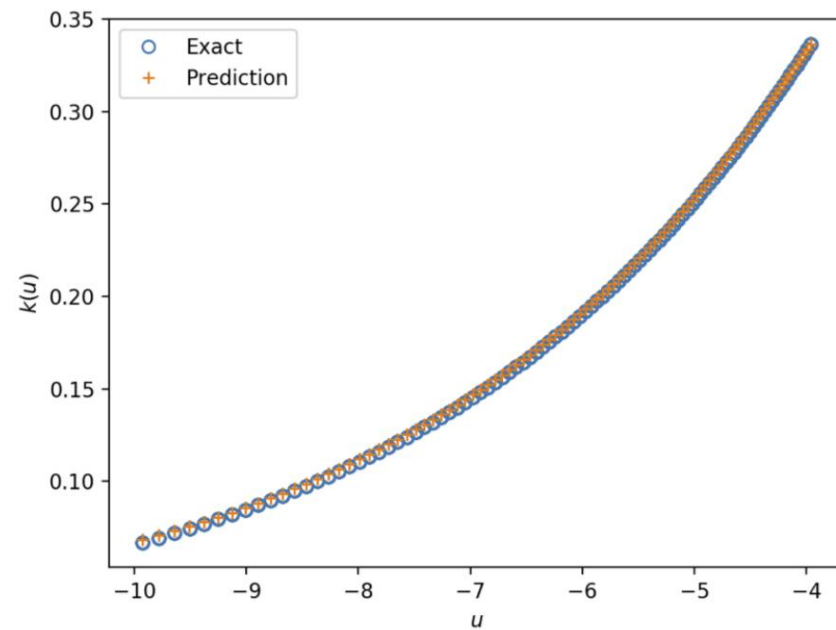


Figure 10: Comparison of the estimated $\hat{K}(u)$ and the reference $K(u)$ given by the van Genuchten model.